JMEPEG (2011) 20:1484–1490
DOI: 10.1007/s11665-010-9785-z

1059-9495/$19.00

Effect of Heat Treatment Temperature on Chemical Compositions of Extracted Hydroxyapatite from Bovine Bone Ash

M. Younesi, S. Javadpour, and M.E. Bahrololoom

(Submitted May 20, 2009; in revised form October 17, 2010)

This article presents the effect of heat treating temperature on chemical composition of hydroxyapatite (HA) that was produced by burning bovine bone, and then heat treating the obtained bone ash at different temperatures in range of 600-1100 °C in air. Bone ash and the resulting white powder from heat treating were characterized by Fourier transformed infrared spectroscopy (FT-IR) and x-ray diffractometry (XRD). The FT-IR spectra confirmed that heat treating of bone ash at temperature of 800 °C removed the total of organic substances. x-ray diffraction analysis showed that the white powder was HA and HA was the only crystalline phase indicated in heat treating product. x-ray fluorescence analyses revealed that calcium and phosphorous were the main elements and magnesium and sodium were minor impurities of produced powder at 800 °C. The results of the energy dispersive x-ray analysis showed that Ca/P ratio in produced HA varies in range of 1.46-2.01. The resulting material was found to be thermally stable up to 1100 °C.

Keywords advanced characterizations, biomaterials, heat treating

1. Introduction

Bones consist of organic (30%) and inorganic compounds (70%). Mineral parts of bones provide their stiffness and proper mechanical properties. Biological apatites are the components of bones and also pathological tissue (urolith, tooth scale, and mineralized soft tissue) (Ref 1-3). Those apatites are nonstoichiometric; in enamel and dentine, the Ca/P molar ratio exceeds 1.67. Due to its chemical and structural similarities to bone minerals, HA is a promising candidate for bone substitutes. HA is not only a biocompatible, osteoconductive, nontoxic, noninflammatory, and nonimmunogenic agent but also is bioactive, i.e., it has got the ability to form a direct chemical bond with living tissues (Ref 4, 5).

It is the most commonly used calcium phosphate in orthopedics as it is osteoconductive (Ref 6). Its production has been well reported (Ref 7-10). There are different methods for synthesis of HA which include precipitation (Ref 11, 12), hydrolysis (Ref 13, 14), and hydrothermal synthesis (Ref 15, 16).

An alternative method for preparation of HA can be its extraction from natural resources. There are a few methods of extracting HA from animal bones: thermal decomposition, subcritical water process, and alkaline hydrolysis (Ref 5, 17). In the research, we applied pork bones after acid hydrolysis. The chemical treatment was carried out using a mild agent, i.e., a solution of lactic acid, and soft conditions, i.e., a temperature of 125-135 °C and the pressure of 0.26-0.30 MPa. Contrary to alkaline hydrolysis, this method eliminates the problem of hazardous alkaline waste management. The final product of the hydrolysis process using lactic acid is apart from bone sludge used for HA extraction, a protein hydrolysate of high purity used in food industry (Ref 18).

In fact, some researchers have attempted to synthesis HA from biological materials. Corals (Ref 19), eggshells (Ref 20, 21), and ostrich eggshells (Ref 22) have also been utilized to produce HA or used as a bone substitute. The main constituent of an eggshell is calcium carbonate (94%) and calcium phosphate (1%). It also has 4% organic compounds and 1% magnesium carbonate. By heating eggshells at 900 °C for 2 h, Rivera et al. (Ref 20) converted the calcium carbonate content of eggshells into calcium oxide via the following equation:

$$CaCO_3 \rightarrow CO_2 + CaO \quad \text{(Eq 1)}$$

Then they added the calcium oxide obtained from eggshells to a tricalcium phosphate solution and heated the mixture to 1050 °C for 3 h to produce HA, according to:

$$3Ca_3(PO_4)_2 + CaO + H_2O \rightarrow Ca_{10}(PO_4)_6(OH)_2 \quad \text{(Eq 2)}$$

Krishna et al. (Ref 21) modified the above process using a microwave oven to produce nanocrystalline HA from eggshells. A group of Korean scientists synthesized calcium phosphate powders from cuttlefish bone (Ref 22). Their process was partly similar to the work reported by Rivera et al. (Ref 20) and produced CaO by burning cuttlefish bone. Another process for preparation of HA and other calcium phosphate materials for biomedical applications can be their extraction from bone, since HA is the main inorganic constituent of natural bone. Hydrothermal synthesis of HA from bovine bone has been reported by Jinawath et al. (Ref 23). In their extensive studies, a group of New Zealand researchers

M. Younesi, S. Javadpour, and **M.E. Bahrololoom**, Department of Materials Science and Engineering, Shiraz University, Shiraz, Iran. Contact e-mail: mousa_younesi_3@yahoo.com.

have used bone to produce orthopedic implants (Ref 24). Through a process of boiling, solvent treatment, and deproteination they converted bovine bone to an implant material. An alternative process in producing HA from bovine bone can be its extraction from bone ash. Two advantages of this process are removal of all organic components of bone and also preventing the possibility of transmission of dangerous diseases. When a piece of bone is burned fully, its organic components are removed. The remaining ash contains the inorganic constituents of the bone. Consequently, bone ash can be used to extract HA. Assuming that the remaining ash can be converted fully to HA, about 1.6 kg compact bone should yield 1 kg HA. Such a process would certainly be an economic method for producing HA to be used as a biomaterial in orthopedic and dental implants.

The aim of the present research was producing the HA from bovine bone ash and investigating the effect of heat treating temperature on chemical composition of produced HA from heat treating of bone ash. Here, different chemical analysis techniques were employed to investigate the structure and composition of the resulting material.

2. Experimental Procedure

2.1 Extraction Process

Different types of bones from different animals were used as the starting materials for this process. Bovine femur bone, sheep femur bone, sheep skull flat bone, chicken femur, and plaice vertebrae were chosen to compare the efficiency of the process for these different types of bone, i.e., the amount of powder obtained per unit weight of bone. This was to find out which type of bone is the best to use regarding the amount of bone ash produced after burning bone. It was found that the highest amount of bone ash powder per unit weight of bone was obtained for bovine femur bone. Bovine tibia, humerus, and ulna were also tested and the results were similar to that obtained for bovine femur. Hence, bovine femur, tibia, humerus, and ulna were chosen as the main starting biological material. The spongy bones were discarded and the bone marrow and all pieces of meat and fat were removed. Using a gas torch and applying direct flame to the cleaned bone, organic components were burned. The product of this thermal process contained some char due to burning of organic components. To remove the remaining char, the black powder (bone ash) was heated in an air furnace at different temperatures between 600 to 1100 °C for 3 h and finally it was cooled inside the furnace. As a result of this process, the black ash was turned into a white powder.

2.2 Chemical Characterization

To investigate the presence of organic species and also the degree of probable dehydroxylation of HA during heat treatment FTIR analysis was performed in the present investigation using a Scimitar Series FTS 2000 Digilab spectrophotometer in the range of middle infrared of 400-4000 cm^{-1}. To record the FTIR spectrum of each sample, 2 mg of the powder was mixed and pressed with 300 mg of KBr to get a pellet for FTIR analysis. A Philips, PW 2400 x-ray fluorescence spectrometer was used to obtain elemental chemical composition of the extracted powder. In order to prepare samples for XRF analysis, the powder was poured into a special die and compacted in a pressing machine with 8 tons pressure to prepare a disk-shaped specimen with 30 mm diameter and 5 mm thickness. Phase composition was analyzed using the x-ray diffraction method by a Philips X'Pert diffractometer equipped with graphite monochromator using Cu Kα 1.54 (40 kV, 40 mA) and recorded from 5° to 60° for 2θ at a scanning speed of 2.5°/min and a step size of 0.02°. The resulted patterns were studied quantitatively by Rietveld analysis which used the fundamental parameter procedure implemented in TOPAS R-version 2.1. For semi-quantitative analysis and to study the Ca/P ratio in the extracted material, a Cambridge S-360 scanning electron microscope (SEM) equipped with an Oxford energy dispersive x-ray (EDX) analyzer working at 15 kV accelerating voltage was used. Ten measurements were performed and it was assumed that the peak height is proportional to the mole fraction of an element.

To evaluate the thermal stability of the extracted material, differential thermal analysis (DTA) and thermogravimetric analysis (TGA) were performed using a Mettler Toledo 851E thermal analyzer by changing the temperature from room temperature to 1200 °C in air at a rate of 5 °C/min. The variability in the signal was 0.25 wt.% for TGA and approximately 5.7×10^{-3} μV/g for DTA. The weight of the sample for thermal analysis was 20 mg and α-Al_2O_3 was used as a crucible and a reference sample.

3. Results and Discussion

3.1 FTIR Analysis

The FTIR spectrum of the bone ash is showed in Fig. 1(a). In this figure, we can see a series of bands in the mid-infrared region; a strong band at 1043 cm^{-1}, another band at 1456 cm^{-1} with a shoulder at 1417 cm^{-1}, and also a small sharp band at 667 cm^{-1}. Comparison of infrared spectra obtained from analysis of bone and bone ash confirm the removal of organic components after burning of bovine bone. The infrared spectrum of bone has been recently reported by Boskey and Camacho shows the presence of the major inorganic species, phosphate and carbonate groups (from HA), and also the organic components such as amide functional groups from the protein constituents of bone, i.e., collagen (Ref 25). Although they recorded infrared absorbance between 800 and 1800 cm^{-1}, nevertheless, comparing their results for bone with the FTIR spectrum obtained for bone ash in this study shows clearly that all organic components of bone have disappeared after burning. The bands associated with the amide groups of proteins in wave numbers 1250, 1560, and 1650 cm^{-1} which are observed on the spectrum of bone do not exist on the FTIR spectrum of bone ash prepared in this study. On the other hand, the bands for phosphate and carbonate groups in bone ash occur at the same wave numbers as those reported for bone. This comparison shows that the procedure of burning bone is perfectly sufficient to remove all organic components of bone. Furthermore, there is no absorption bands related to C-H bonds in the FTIR spectrum of the bone ash. This indicates that heat treating of the bone ash lead to total removal of the organic materials of bone (Ref 26). Therefore, all bands observed in the FTIR of Fig. 1(a) are related to the inorganic components of bone which were

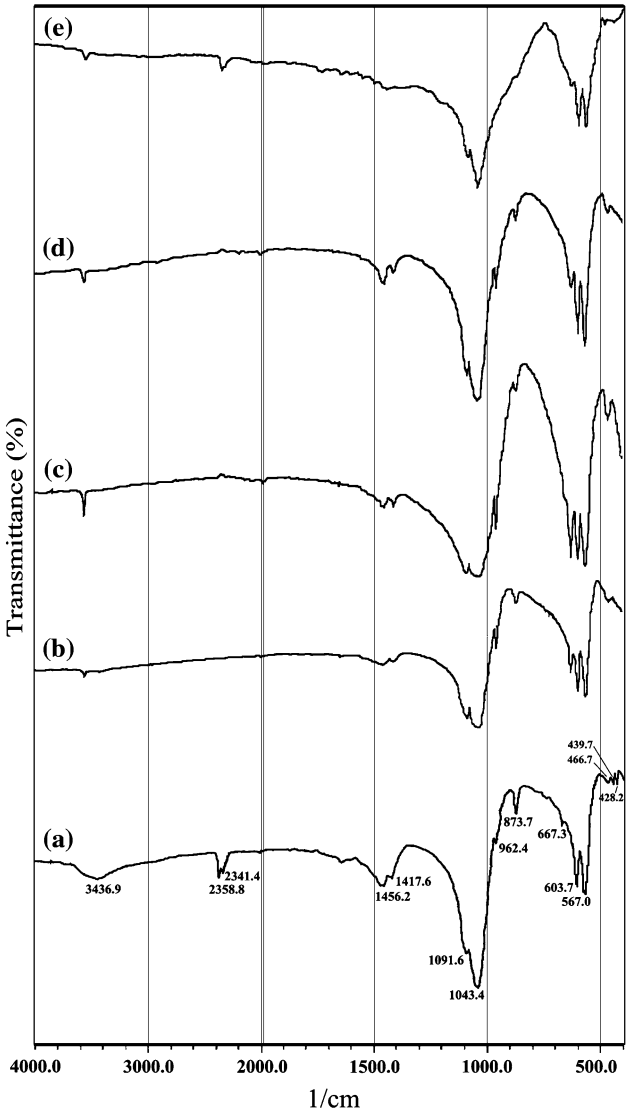

Fig. 1 The FTIR spectrum of the bone ash (a) and samples of bone ash heat treated at (b) 600 °C, (c) 700 °C, (d) 800 °C, and (e) 1100 °C

presented in the bone ash. We can divide these bands into three main categories; phosphate bands, carbonate bands, and hydroxyl group bands. One strong and relatively broad band at 1043 cm^{-1}, two relatively strong and sharp bands at 567 and 603 cm^{-1}, and another band at 962 cm^{-1} which appear on the FTIR spectrum of Fig. 1(a) are related to the phosphate group. Tanaka et al. also observed two bands at 603 and 1051 cm^{-1} due to the stretching vibrations of the phosphate group (Ref 27). The bands which appear at 873, 1417, and 1456 cm^{-1} are associated with the carbonate group. The carbonate ion can competitively replace at two sites in the apatite structure, the hydroxyl and the phosphate ion positions, giving A- and B-type carbonated apatite, respectively. These two types of substitution can occur simultaneously, resulting in a mixed AB-type substitution which forms bone mineral. Therefore, the peak position of carbonate ions in FTIR spectra depends on whether the carbonate ion is substituted for the hydroxyl ion or the phosphate ion in the HA lattice. There is also a relatively broad band at 3436 cm^{-1} which is attributed to the hydroxyl group.

The FTIR spectra of bone ash samples which were heat treated at 600, 700, 800, and 1100 °C are presented in Fig. 1(b-e). They provide a number of spectral details indicating some changes have occurred by increasing the temperature of heat treating. The band at 2341 cm^{-1} has disappeared after heat treating bone ash which might be because of the elimination of carbon in the bone ash in the form of carbon dioxide gas in presence of air oxygen. This is in agreement with the change of color of the bone ash powder from black to white after heat treating. The broad band at 3436 cm^{-1} observed in the spectrum of Fig. 1(a) has almost disappeared and replace by a small peak at 3571 cm^{-1} in the spectra of Fig. 1(b-e), which is caused by the carboxyl stretching. Brinov et al. (Ref 28) have recently investigated the effect of sintering temperature on the FTIR of carbonated HA and reported that the band at 3570 cm^{-1} due to the hydroxyl group stretch mode disappeared after sintering HA at 1100 and 1500 °C. It was found here that as the heat treating temperature increases up to 1100 °C, the band at 634.5 cm^{-1} which originates from vibration of the hydroxyl ion is very sensitive to temperature and disappears, while the band at 3571.9 cm^{-1} which corresponds to the stretching vibration bands of the hydroxyl ion is more stable and become broader. This is because of the dehydroxylation of HA which may occur at temperatures above 850 °C. The results of these FTIR analyses show that heat treating of the bone ash above 800 °C can cause dehydroxylation of the HA. The FTIR spectrum of the sample which was heat treated at 800 °C (Fig. 2d) is in good agreement with the spectra reported by Markovic et al. (Ref 9) for a HA-synthetic reference material (HA-SRM). In this figure, the stretching band at 3571 cm^{-1} and vibration band at 634 cm^{-1} are created by OH^- groups. The bands located at 474, 570, 603, 962, 1049, and 1089 cm^{-1} originated by PO_4^{3-} ions (Ref 9, 26, 29). The intensity of O-H stretching vibration in HA is weaker than strong P-O stretching vibration due to HA stoichiometry. The bands at 873.7, 1415.7, and 1456.2 cm^{-1} are originated by CO_3^{2-} ions. Carbonate ions are a common impurity in both synthetic HA and HA produced from natural resources (Ref 9, 26, 29). The results of FTIR analyses in the present research showed that the best heat treating temperature for the conversion of bone ash to HA was 800 °C. Therefore, the optimum temperature for heat treating of bone ash was found to be 800 °C.

3.2 XRF Analysis

Table 1 presents the results of XRF analysis of the HA produced from heat treating of the bone ash at temperature of 800 °C. Also, the chemical composition of this material in oxide form is shown in Table 2. As seen, calcium and phosphorous are the main components, and magnesium and sodium are minor elements, and also some traces of potassium and strontium are present. As seen in Table 2, the concentrations of CaO and P_2O_5 are 54.079 and 42.860 wt.%, respectively. The elemental chemical analysis of HA extracted from bovine bone by the Merck Chemicals (Endobon) has also been reported by Joschek et al. (Ref 29) and their investigation resulted in identifying numerous elements. This huge number of elements is not astonishing to the well accepted since ion exchange can take place in the apatite component of bone. The ionic components of HA, i.e., Ca^{2+}, OH^-, and PO_4^{3-} can readily be exchanged by other ions. It is obvious that the composition of the trace elements varies considerably in bone depending on some biological factors such as nutrition

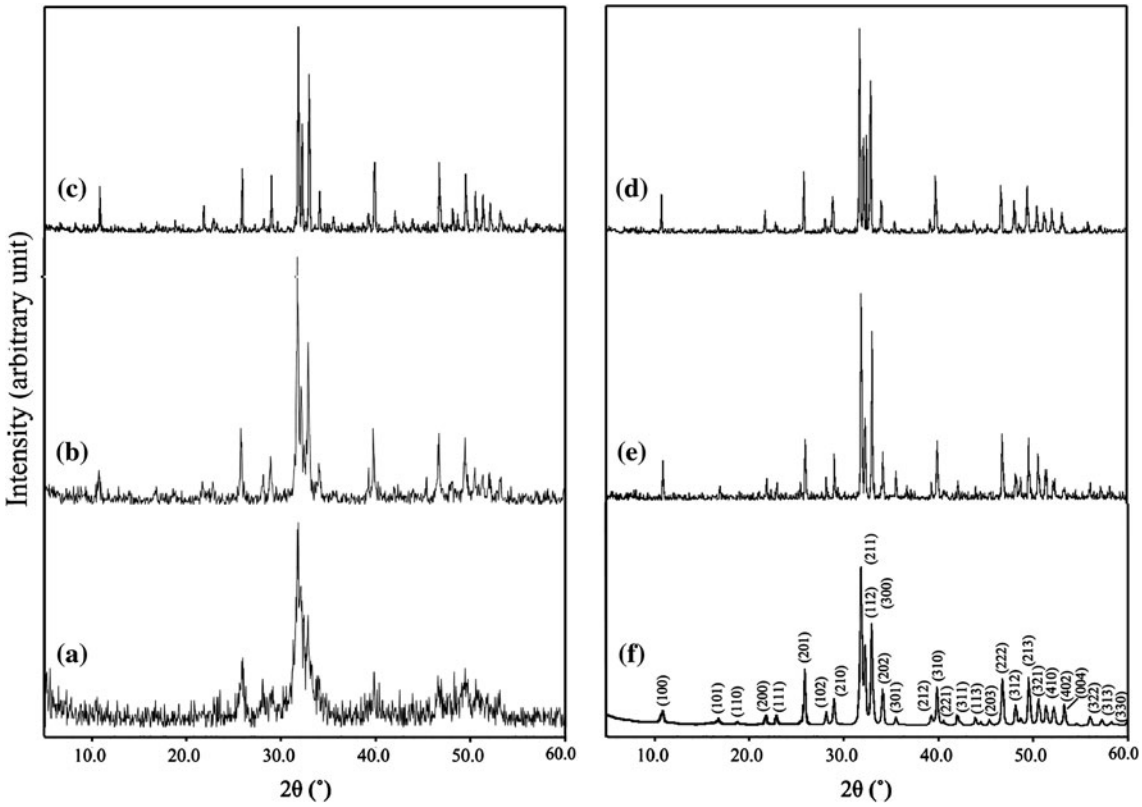

Fig. 2 XRD patterns of bone ash (a) and its heat treated forms produced at different temperatures; 600 °C (b), 700 °C (c), 800 °C (d), and 1100 (e). (f) XRD pattern that is related to standard hydroxyapatite (NIST, SRM-2910)

Table 1 Elemental composition (XRF analysis) of the NHA, heat treated at 800 °C

Elements	Concentration, wt.%	Absolute error, %
Ca	64.92	0.07
P	31.53	0.05
Na	1.91	0.01
Mg	1.36	0.01
Sr	0.086	0.002
K	0.091	0.003

Table 2 Composition of the HA, heat treated at 800 °C, in oxide form

Compounds	Concentration, wt.%	Absolute error, %
CaO	54.079	0.060
P_2O_5	42.860	0.050
MgO	1.343	0.020
Na_2O	1.530	0.030
K_2O	0.065	0.002
SrO	0.061	0.002

(Ref 29). The chemical compositions of synthetic HA and also HA extracted from pig and bovine bones were compared with each other in the work of Haberko et al. (Ref 26). They found that calcium, phosphorus, and magnesium contents (in oxide forms) of HA extracted from bovine bone were CaO: 52.25 wt.%, P_2O_5: 38.37 wt.%, and MgO: 0.41 wt.%. It can be seen that the results of Table 2 are in good agreement with these results. The concentration of magnesium determined by XRF analysis of the study made here was found to be 1.36 wt.% which is higher than the value of magnesium content quoted by Haberko et al. (Ref 26) which was reported to be 0.41 wt.%. This discrepancy might be due to the type of bovine bone which was used here as the starting material for producing HA. The bones were purchased from the local slaughter-house and there was no information about the breed and exact age of the cattle from which the bones were supplied. Breed and age of the animal can be influential parameters determining the composition of HA in their calcified tissues.

3.3 XRD Analysis

Figure 2 shows the XRD patterns of the black powder produced after burning bone, i.e., the bone ash (a) and its heat treated forms produced at 600 °C (b), 700 °C (c), 800 °C (d), and 1100 °C (e). These diffraction patterns show a gradual increase in the degree of sharpness of peaks with increasing heat treating temperature, indicating the extent of crystallinity of HA produced at various temperatures. The diffraction pattern (Fig. 2a) of the bone ash is very broad which indicates the presence of small crystals of HA. Other diffraction patterns of Fig. 2(b-e) show patterns which are narrow and sharp when compared with the pattern of the bone ash before heating. The resulted sharpening of the XRD pattern of the heat treated bone ash could be due to change in the crystal size of the powder. Similar observations have been reported by Shipman et al. (Ref 30) and they explained results of XRD patterns in terms of alteration in crystal size. They found that there was a gradual

increase in HA crystal size associated with increased heat treating temperature (Ref 30). The black powder, produced in this study, began recrystallization at about 600 °C without decomposing to any other compound of the calcium phosphate family. Peaks which would indicate the thermal decomposition of HA into α-tricalcium phosphate and tetracalcium phosphate were not observed at any temperature up to 800 °C. Sharp clear reflections observed after heat treating at 800 °C correspond to HA and this confirms the phase purity and high crystallinity of HA produced after heat treating the bone ash at this temperature. Lee et al. (Ref 22) also reported fully crystallized HA at 900 °C when they synthesized HA from calcined cuttlefish bone. Figure 2(e) shows the appearance of a low intensity peak at 2θ of 31.1° corresponding to β-tricalcium phosphate. Keeping the powder at 1100 °C for 3 h resulted in this peak with low intensity, whereas heating the bone ash at temperatures lower than 1100 °C did not give any indication of the presence of β-tricalcium as an impurity phase. As mentioned, crystallite size influences peak broadening. It should be noted that XRD analysis only provides a spatial average of crystallite size estimates. Thus, changes in peak broadening represent changes to the crystallite size distribution. There are some chemical factors which affect the crystallite size. These include denaturing of the bone matrix during burning through release of water, in which the mineral crystals recrystallize, and removal of the collagen fibril networks which influence crystallite size of the bone ash, as seen in Fig. 2(a). Figure 2(f) shows a XRD pattern that is related to standard HA (NIST, SRM-2910) (Ref 31). A comparison between Fig. 2(d) that produced at temperature of 800 °C with Fig. 2(f) which is related to HA-SRM 2910 indicates that these two pattern are completely similar and both of them are in full agreement with the corresponding values reported for hexagonal HA (JCPDS, Card No. 9-432) (Ref 32).

The results of the quantitative analysis which have been calculated by the use of Rietveld analysis is presented in Fig. 3 and chemical composition of the HA from quantitative analysis of the XRD spectra is shown in Table 3. These results indicate that this HA contains some $NaCaPO_4$, CaO, and MgO as impurities. They are in good agreement with the results of the XRF analysis (Table 1, 2), where Na and Mg were detected as the minor impurity elements. The content of CaO was found to be 1 wt.% (Table 3). It should be appreciated that low concentrations of CaO are advantageous because the presence of CaO reduces the biocompatibility of HA (Ref 26). The work of Joschek et al. (Ref 29) on characterization of HA produced from animal bone, Endobon, indicated the presence of MgO, CaO, $Ca_4O(PO_4)_2$ and $NaCaPO_4$ as impurity phases. Moreover, when bone ash is heated at temperatures higher than about 1200 °C tricalcium phosphate and tetracalcium phosphate are formed due to phase transformation of HA at high sintering temperatures. These two phases are not present in the HA extracted from bone ash in this study because the optimum heat treating temperature which was found here (800 °C) is lower than the phase transformation temperature of HA to other calcium phosphate phases.

3.4 Study of Ca/P Ratio with EDX

The results of the EDX analysis (Fig. 4) showed that the Ca/P ratio of HA investigated in this study is about 1.67.

Table 3 Chemical composition of NH from quantitative analysis of the XRD spectra

Component	2θ value, °	Content, wt.%
$NaCaPO_4$	33.7	2
CaO	37.4	1
MgO	42.9	1
Hydroxyapatite	31.8	96

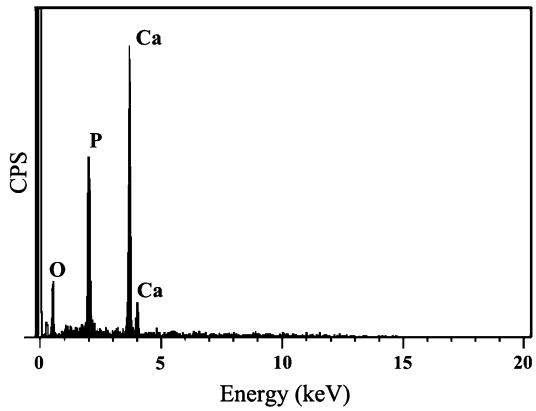

Fig. 4 The EDX analysis of produced HA powder at temperature of 800 °C

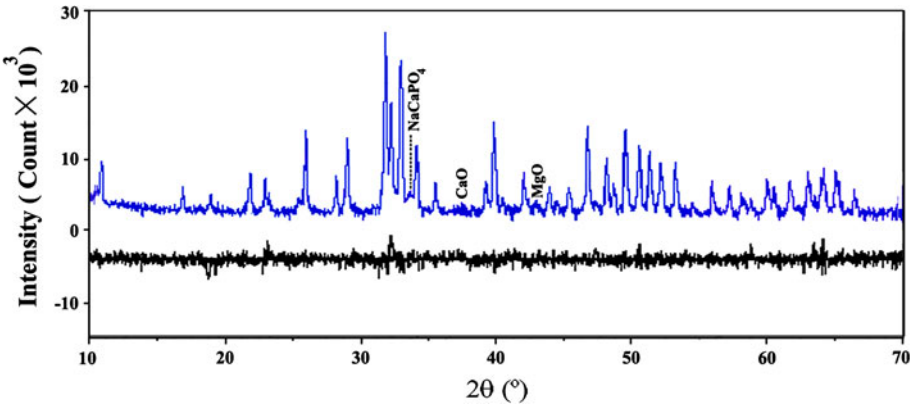

Fig. 3 Quantitative analysis of the XRD pattern of produced HA at 800 °C

The Ca/P ratio found in the present investigation agrees with the values reported by Lee et al. (Ref 22). The essential difference between synthetic and HA produced from bovine bone is that the latter showed a higher Ca/P ratio than the synthetic material, while the former was closer to the stoichiometric HA (Ref 26, 29). It should be noted that there is a technical problem with the semi-quantitative analysis of Ca/P ratio of HA by the use of EDX. In other words, during the analysis at a fixed current density and increasing irradiation time, the x-ray intensity of phosphorus decreases more rapidly than that of calcium leading to an increase of the Ca/P ratio at a high electron irradiation dose. Thus, in this study, the accelerating voltage was set at 15 kV and the analysis was performed at a low irradiation time to overcome the above mentioned problem.

3.5 DTA-TGA

The results of differential thermal analysis (DTA) and thermogravimetric analysis (TGA) of NHA are shown in Fig. 5. A small weight loss was detected by TGA and a small endothermic transition was observed in the DTA at low temperatures (<150 °C). The endothermic reaction at low temperatures is attributed to evaporation of adsorbed water (Ref 26, 28, 29). Furthermore, by attention to TGA-curve in Fig. 5, we can see an initial mass loss in the temperature range from 30 to 100 °C and a mass loss in the range from 100 to 250 °C. These two losses correspond to mainly physisorbed water although some chemisorbed water is also expected to be lost between 100 and 250 °C. Between 250 and 850 °C, some mass loss was observed which corresponds to chemisorbed water. These behaviors are in agreement with the achieved results of Rootare and Craige (Ref 33).

Hu et al. investigated thermal analysis of coral, as a part of their study to produce hydoxyapatite from coral, and reported that thermal analysis of coral shows three regions of weight loss. The endothermic loss at 50-140 °C corresponds to the evaporation of absorbed water. Also, two other regions were attributed to the exothermic losses at 150-450 °C to the removal of organic compounds in coral and the endothermic loss at 600-750 °C to the decomposition of calcium carbonate to calcium oxide (Ref 34). Olsen et al. (Ref 35) have also suggested that heating of bones results in weight losses at temperatures lower than 225 °C (due to water evaporation), at temperatures between 225 and 500 °C (caused by the combustion of the organic components of bone) and at temperatures higher than 500 °C (as a result of the decomposition of structural carbonate by release of CO_2 gas). The exothermic losses at 150-450 °C, observed by Hu et al. (Ref 34) which is related to the removal of organic compounds in coral, or at 225-500 °C, reported by Olsen et al. (Ref 28) due to the removal of organic components of bone, was not observed in the DTA-TGA curves of this study. In this study, organic components of bone were removed completely during heating bone to produce bone ash as confirmed by the previous discussion of FTIR analysis. Furthermore, weight loss at high temperatures (800-1200 °C) can be because of partial dehydroxylation of HA (Ref 29). The DTA curve shows an endothermic reaction in this temperature range (800-1200 °C) that can be related to dehydroxylation process of HA powder. This dehydroxylation was also confirmed by the results of FTIR study, as seen in Fig. 2(d) and (e). Thus, the results of DTA-TGA in this study indicated that the HA produced here is stable up to 1100 °C. It should be mentioned that when the bone ash was heated at 1100 °C for 3 h, a peak with low intensity attributed to β-tricalcium phosphate just began to appear as discussed previously in Fig. 2. Haberko (Ref 26) reported exothermic transition due to decomposition of $CaCO_3$ in the DTA curve of HA extracted from pig bone. They showed that by heat treating the material at 700 °C and at higher temperatures the concentration of carbonate groups decreased and as a result, one peak corresponding to CaO appear in their XRD pattern. Also, their results showed that for the sample heat treated at 800 °C the concentration of carbonate groups and also CaO is very low, ~2 and ~0.1%, respectively. Dissociation of calcium carbonate at temperatures between 400 and 600 °C in air has been reported by some researchers (Ref 29, 34). Presence of carbonate groups in HA was detected by FTIR analysis. During heat treating of the bone ash at 800 °C for 3 h, carbonate groups were decomposed and their concentrations were decreased which resulted in the formation of 1% CaO in the XRD spectra. These results are in agreement with results of other researcher (Ref 26, 29, 34). The results of this DTA-TGA study indicated that HA produced here has satisfactory thermal stability up to 1100 °C.

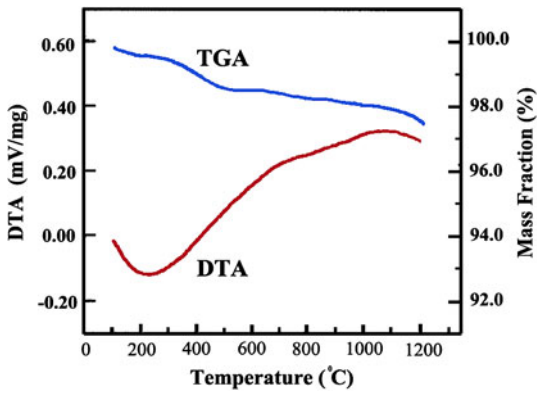

Fig. 5 The DTA-TG curves of produced HA at temperature of 800 °C

4. Conclusions

In this study, we investigate the effect of heat treatment temperatures on chemical composition of HA that was produced from heat treatment of bone ash. The results of this study showed that the optimum heat treating temperature to prevent phase transformation of HA prepared from bone ash is 800 °C. The results of FTIR analyses showed that heat treated bone ash at temperatures lower than 800 °C leave some impurities in HA produced from bovine bone. In addition, results of DTA-TGA analyses indicated that this HA is stable at temperatures lower than 1100 °C. As the basic result of all the analyses which were done in present investigation, the best heat treating temperature for producing HA from bovine bone ash is 800 °C.

Acknowledgment

The authors thank Shiraz University Research Council for financial support through Grant number 87-GR-ENG-62.

References

1. V.P. Orlovskii, V.S.M. Komlev, and S.M. Barinov, Hydroxyapatite and Hydroxyapatite-Based Ceramic, *Inorg. Mater.*, 2002, **38**, p 973–984
2. Z. Knychalska-Karwan and A. Slosarczyk, *Hydroksyapatyt Stomatologii*, Krakmedia, Kraków, 1994
3. M. Vallet-Regi and J.M. Gonzalez-Calbet, Calcium Phosphates as Substitution of Bone Tissues, *Prog. Solid State Chem.*, 2004, **32**, p 1–31
4. M.H. Fathi, A. Hanifi, and V. Mortazavi, Preparation and Bioactivity Evaluation of Bone-Like Hydroxyapatite Nanopowder, *J. Mater. Process. Technol.*, 2008, **202**, p 536–542
5. N.A.M. Barakat, M.S. Khil, A.M. Omran, F.A. Sheikh, and H.Y. Kim, Extraction of Pure Natural Hydroxyapatite from the Bovine Bones Biowaste by Three Different Methods, *J. Mater. Process. Technol.*, 2009, **209**(7), p 3408–3415
6. L.D. Dorr, Z. Wan, M. Song, and A. Ranawat, Bilateral Total Hip Arthroplasty Comparing Hydroxyapatite Coating to Porous Fixation, *J. Arthroplasty*, 1998, **13**, p 729–736
7. S.W.K. Kweh, K.A. Khor, and P. Cheang, The Production and Characterization of Hydroxyapatite (HA) powders, *J. Mater. Proc. Technol.*, 1999, **89–90**, p 373–377
8. L. Bernard, M. Freche, J.L. Lacout, and B. Biscans, Preparation of Hydroxyapatite by Neutralization at Low Temperature—Influence of Purity of the Raw Material, *Powder Technol.*, 1999, **103**, p 19–25
9. M. Markovic, B.O. Fowler, and M.S. Tung, Preparation and Comprehensive Characterization of a Calcium Hydroxyapatite Reference Material, *J. Res. Natl Inst. Stand. Technol.*, 2004, **109**, p 553–568
10. A. Tampieri, G. Celotti, S. Sprio, A. Delcogliano, and S. Franzese, Porosity-Graded Hydroxyapatite Ceramics to Replace Natural Bone, *Biomaterials*, 2001, **22**, p 1365–1370
11. M. Asada, Y. Miura, A. Osaka, K. Oukami, and S. Nakamura, Hydroxyapatite Crystal Growth on Calcium Hydroxyapatite Ceramics, *J. Mater. Sci.*, 1988, **23**, p 3202–3205
12. M. Jarcho, C.H. Bolen, M.B. Thomas, J. Bobic, J.F. Kay, and R.H. Doremus, Hydroxylapatite Synthesis and Characterization in Dense Polycrystalline Form, *J. Mater. Sci.*, 1976, **11**, p 2027–2035
13. H. Monma and T. Kaymiya, Preparation of Hydroxyapatite by the Hydrolysis of Brushite, *J. Mater. Sci.*, 1987, **22**, p 4247–4250
14. D.M. Liu, T. Troczynski, and D. Hakimi, Effect of Hydrolysis on the Phase Evolution of Water-Based Sol–Gel Hydroxyapatite and its Application to Bioactive Coatings, *J. Mater. Sci. Mater. Med.*, 2002, **13**, p 657–665
15. E. Sada, H. Kumazama, and Y. Murakami, Hydrothermal Synthesis of Crystalline Hydroxyapatite Ultrafine Particles, *Chem. Eng. Commun*, 1991, **103**, p 57–64
16. H. Takeo, H. Yasuhiko, and Y. Murakami, Hydrothermal Synthesis of Hydroxyapatite from Calcium Pyrophosphate, *J. Mater. Sci. Lett.*, 1989, **8**, p 305–306
17. C.Y. Ooi, M. Hamdi, and S. Ramesh, Properties of Hydroxyapatite Produced by Annealing of Bovine Bone, *Ceram. Int.*, 2007, **33**, p 1171–1177
18. Z. Kowalski, Z. Wzorek, K. Krupa-Zuczek, M. Konopka, and A. Sobczak, The Possibilities of Obtaining Hydroxyapatite from Meat Industry, *Mol. Cryst. Liquid Cryst.*, 2008, **486**, p 282–290
19. I. Manjubala, M. Siva Kumar, T.S. Sampath Kumar, and K. Panduranga Rao, Synthesis and characterization of functional gradient materials using Indian corals, *J. Mater. Sci. Mater. Med.*, 2000, **11**, p 705–709
20. E.M. Rivera, A. Araiza, W. Brostow, V.M. Castano, J.R. Diaz-Estrada, R. Hernandez, and J. Rogelio Rodriguez et, Synthesis of Hydroxyapatite from Eggshells, *Mater. Lett.*, 1999, **41**, p 128–134
21. D.S.R. Krishna, A. Siddharthan, S.K. Seshadri, and T.S. Sampath Kumar, A Novel Route for Synthesis of Nanocrystalline Hydroxyapatite from Eggshell Waste, *J. Mater. Sci. Mater. Med.*, 2007, **18**, p 1735–1743
22. S.J. Lee, Y.C. Lee, and Y.S. Yoon, Characteristics of Calcium Phosphate Powders Synthesized from Cuttlefish Bone and Phosphoric Acid, *J. Ceram. Process. Res.*, 2007, **8**(6), p 427–430
23. S. Jinawath, D. Pongkao, and M. Yoshimura, Hydrothermal Synthesis of Hydroxyapatite from Natural Source, *J. Mater. Sci. Mater. Med.*, 2002, **13**, p 491–494
24. G.S. Johnson, M.R. Mucalo, and M.A. Lorier, The Processing and Characterization of Animal-Derived Bone to Yield Materials with Biomedical Applications. Part II: Milled Bone Powders, Reprecipitated Hydroxyapatite and the Potential Uses of These Materials, *J. Mater. Sci. Mater. Med.*, 2000, **11**, p 427–441
25. A. Boskey and N.P. Camacho, FT-IR Imaging of Native and Tissue-Engineered Bone and Cartilage, *Biomaterials*, 2007, **28**, p 2465–2478
26. K. Haberko, M.M. Bucko, J. Brzezinska-Miecznik, M. Haberko, W. Mozgawa, T. Panz, A. Pyda, and J. Zarebski, Natural Hydroxyapatite—Its Behaviour During Heat Treatment, *J. Eur. Ceram. Soc.*, 2006, **26**, p 537–542
27. Y. Tanaka, Y. Hirata, and R. Yoshinaka, Synthesis and Characteristics of Ultrafine Hydroxyapatite Particles, *J. Ceram. Process. Res.*, 2003, **4**(4), p 197–201
28. S.M. Barinov, J.V. Rau, S.N. Cesaro, J. Durisin, I.V. Fadeeva, D. Ferro, L. Medvecky, and G. Trionfetti, Carbonate Release from Carbonated Hydroxyapatite in the Wide Temperature Rage, *J. Mater. Sci. Mater. Med.*, 2006, **17**, p 597–604
29. S. Joschek, B. Nies, R. Krotz, and A. Gopferich, Chemical and Physicochemical Characterization of Porous Hydroxyapatite Ceramics Made of Natural Bone, *Biomaterials*, 2000, **21**, p 1645–1658
30. P. Shipman, G. Foster, and M. Schoeninger, Burnt Bones and Teeth: an Experimental Study of Color, Morphology, Crystal Structure and Shrinkage, *J. Archaeol. Sci.*, 1984, **11**, p 307–325
31. Certificate of Analysis, Standard Reference Material 2910, National Institute of Standards and Technology, Gaithersburg, MD, USA (1997)
32. Powder Diffraction File: Inorganic Phases, Joint Committee on Powder Diffraction Standards, Swarthmore (1986) Card No. 9-432
33. H.M. Rootare and R.G. Craig, Vapor Phase Adsorption of Water on Hydroxyapatite, *J. Dent. Res.*, 1977, **56**(12), p 1437–1488
34. J. Hu, J.J. Russell, B. Ben-Nissan, and R. Vago, Production and Analysis of Hydroxyapatite from Australian Corals Via Hydrothermal Process, *J. Mater. Sci. Lett.*, 2001, **20**, p 85–87
35. J. Olsen, J. Heinemeier, P. Bennike, C. Krause, K.M. Hornstrup, and H. Thrane, Characterisation and Blind Testing of Radiocarbon Dating of Cremated Bone, *J. Archaeol. Sci.*, 2008, **35**, p 791–800